APL Bioengineering ARTICLE pubs.aip.org/aip/apb

Highly functional duodenal stent with photosensitizers enables photodynamic therapy for metabolic syndrome treatment: Feasibility and safety study in a porcine model

Cite as: APL Bioeng. **8**, 036103 (2024); doi: 10.1063/5.0206328
Submitted: 1 March 2024 · Accepted: 11 June 2024 ·
Published Online: 2 July 2024

View Online Export Citation CrossMark

Chan Su Park,[1] Hyun Jin Park,[2] Ji Hoon Park,[3] Jin Hee Lee,[2] Hyun Jung Kee,[2] Jung-Hoon Park,[4] Jung Hyun Jo,[2] Hee Seung Lee,[2] Cheol Ryong Ku,[5] Jeong Youp Park,[2] Seungmin Bang,[2] Jung Min Song,[6] Kun Na,[7,8,9] Sung Kwon Kang,[10] Hwoon-Yong Jung,[4] and Moon Jae Chung[2,a)]

AFFILIATIONS

[1]Division of Gastroenterology, Department of Internal Medicine, National Health Insurance Service Ilsan Hospital, Goyang, Korea
[2]Division of Gastroenterology, Department of Internal Medicine, Yonsei Institute of Gastroenterology, Yonsei University College of Medicine, Seoul, Korea
[3]Department of Internal Medicine, Yongin Severance Hospital, Yonsei University College of Medicine, Yongin-si, Korea
[4]Department of Internal Medicine, Asan Medical Center, University of Ulsan College of Medicine, Seoul, Korea
[5]Division of Endocrinology, Department of Internal Medicine, Yonsei Institute of Endocrinology, Yonsei University College of Medicine, Seoul, Korea
[6]Medical Device Team, Medical Device Assessment Headquarters, Korea Testing and Research Institute, Seoul, Korea
[7]Department of Internal Medicine, Seoul St. Mary's Hospital, College of Medicine, The Catholic University of Korea, Seoul, Korea
[8]Department of Biotechnology, The Catholic University of Korea, Gyeonggi, Korea
[9]Department of Biomedical-Chemical Engineering, The Catholic University of Korea, Gyeonggi, Korea
[10]Research and Development Department, S&G Biotech, Gyeonggi, Korea

Note: This paper is part of the special issue on Structure and Mechanics of Biofluids, Biomaterials, and Biologics.
[a)]**Author to whom correspondence should be addressed:** MJCHUNG@yuhs.ac. **Tel.:** +82-2-2228-1981. **Mobile:** +82-10-2953-1088. **Fax:** +82-2-2227-7900

ABSTRACT

Duodenal mucosal resurfacing (DMR) by thermal ablation of the duodenal mucosa is a minimally invasive endoscopic procedure for controlling metabolic syndrome (MS). However, thermal energy can cause adverse effects due to deep mucosal injury, necessitating an additional mucosal lifting process, which complicate the procedures. Therefore, we aimed to develop a similar procedure using non-thermal photodynamic therapy (PDT) for DMR using a highly functional metal stent covered with photosensitizers (PSs) to minimize the potential risks of thermal ablation injury. We developed a novel PS stent enabling the controlled release of radical oxygen species with specific structures to prevent stent migration and duodenal stricture after ablation and performed an animal study (n = 8) to demonstrate the feasibility and safety of PDT for DMR. The stents were placed for 7 days to prevent duodenal strictures after PDT. To confirm PDT efficacy, we stained for gastric inhibitory polypeptide (GIP) and glucose transporter isoform 1. The PS stents were deployed, and PDT was applied without evidence of duodenal stricture, pancreatitis, or hemorrhage in any of the pigs. Microscopic evaluation indicated apoptosis of the mucosal cells in the irradiated duodenum on days 7 and 14, which recovered after day 28. Immunohistochemistry revealed suppressed GIP expression in the mucosal wall of the irradiated duodenum. Endoscopic PDT for DMR using PS stents could be applied safely in a porcine model and may result in decreased GIP secretion, which is a crucial mechanism in MS treatment. Further clinical studies are required to explore its safety and efficacy in patients with MS.

INTRODUCTION

Metabolic syndrome (MS) is a complex disorder defined by a cluster of interconnected factors that increase the risk of coronary heart disease, other forms of cardiovascular atherosclerotic disease, and type 2 diabetes mellitus (T2DM).[1] The prevalence of MS is increasing owing to lifestyle changes that lead to obesity. For example, >20% of the participants in the Third National Health and Nutrition Examination Survey had MS.[2] Furthermore, the number of patients with T2DM worldwide is expected to increase by 51%, from 578×10^6 in 2019 to 700×10^6 in 2045, particularly in Africa and East Asia.[3]

According to the National Cholesterol Education Program Adult Treatment Panel III guidelines, MS treatment involves improving the underlying metabolic abnormalities, which can be achieved through lifestyle modifications and medications.[4] However, bariatric surgery has been used to control blood sugar levels and obesity by suppressing the secretion of incretin hormones or allowing food to bypass the duodenum.[5] Concordantly, this surgery has demonstrated stronger effects on blood sugar metabolism in numerous clinical studies.[5,6] Carlsson *et al.* have reported that T2DM incidence was 28.4 cases and 6.8 cases per 1000 person-years in the control and bariatric surgery groups, respectively.[5] Schauer *et al.* have demonstrated that patients undergoing this surgery showed better weight loss and blood sugar control results. Moreover, the Homeostatic Model Assessment of Insulin Resistance evaluation showed a significant improvement in bariatric surgery patients than in those receiving medical therapy.[6] However, only 1% of the eligible patients with severe obesity requiring surgery undergo this surgery because of various patient factors, including psychological aversion to surgery and inability to tolerate general anesthesia.[7] Furthermore, bariatric surgery is invasive and causes irreversible anatomical changes accompanied by adverse events, such as chronic dumping syndrome, dilation of the esophagus, obstruction of the stomach, and malnutrition. Thus, endoscopic procedures are emerging as an effective and minimally invasive approach to manage obesity and diabetes, narrowing the gap between pharmacological therapy combined with lifestyle modifications and invasive bariatric surgery.[8,9]

Researchers have attempted to develop endoscopic bariatric and metabolic therapies (EBMTs), which are classified into gastric and small bowel categories. Notably, the duodenum has attracted attention as a potential target of EBMT.[10] Thermal ablation of the duodenal mucosa is reportedly a minimally invasive endoscopic procedure that controls hyperglycemia. Duodenal mucosal resurfacing (DMR) was designed to treat insulin resistance-associated metabolic diseases, including T2DM and nonalcoholic fatty liver disease/nonalcoholic steatohepatitis, by targeting the duodenal mucosa.[11] The first-in-human safety trial demonstrated that DMR is safe and can improve glycemic control proportionally to the length of the ablated duodenal mucosal segment.[12–14] The subsequent multicenter, open-label REVITA-1 trial in 46 patients with poorly controlled T2DM reported a significant reduction in the baseline glycated hemoglobin (HbA1c) levels 24 weeks after hydrothermal DMR.[15] The REVITA-2 trial, a prospective, double-blind, sham-controlled study, demonstrated the safety and efficacy of hydrothermal DMR in patients with T2DM.[16] The DMR procedure was well tolerated, safe, and elicited clinically and statistically significant improvements in the HbA1c levels and liver fat content compared with the sham procedure. However, severe adverse events were noted, such as hematochezia and bowel perforation.[16] The risks of severe side effects of deep mucosal injury are inevitable upon using thermal energy. Therefore, thermal energy use necessitates an additional mucosal lifting process, which complicates the procedure. Furthermore, DMR methods using lasers, pulsed electric fields, radio frequency, steam, and cryoablation have been developed for other sites, such as the Barrett's esophagus; however, they are in pre-clinical trial stages and require procedural development for clinical application to humans.[17]

Endoscopic DMR should exhibit a narrow range of toxicity to minimize its effects on other cells in the duodenum. Therefore, non-thermal ablation is considered a more appropriate method for DMR. Photodynamic therapy (PDT) requires a special photosensitizer (PS) and light to induce apoptosis. The application of a specific light wavelength to a photosensitizing agent generates reactive oxygen species (ROS) that can cause damage to cell DNA. Notably, PDT effectively leads to cell apoptosis in diseased tissues without the use of thermal energy. Moreover, PDT has been used for cancer treatment in various organs and skin diseases.[18–20] Concordantly, endoscopic PDT is a safe and feasible method for implementing non-thermal DMR.

The incretin hormones, such as gastric inhibitory polypeptide (GIP) and glucagon-like peptide-1 (GLP-1), are responsible for appetite, food intake, and postprandial insulin secretion. Glucose transporter 1 (GLUT1) is responsible for constitutive glucose uptake. In many organs, GLUT1 is concentrated in the endothelial cells of blood–tissue barriers. Thus, GLUT1 shuttles glucose between the blood and organs. It can lower blood sugar and prevent fat accumulation. However, GIP secreted by the duodenal K-cells has a different effect on patients. In fact, GIP normally has an insulinotropic effect, but in obese patients with high plasma GIP levels, it promotes glucagon secretion (related to high blood glucose) and fat accumulation in the blood vessels and adipocytes.[21,22] Roux-en-Y gastric bypass (RYGB), an effective T2DM treatment method for patients with obesity,[23,24] induces apical and basolateral membrane GLUT1 expression in the small intestinal enterocytes, resulting in increased serum glucose excretion in the gut lumen.[25] The duodenum and a part of the jejunum are bypassed by the RYGB procedure, resulting in a lack of exposure of the K-cells to nutrients and, consequently, reduced secretion of GIP. We have already confirmed these results in the high fat diet–diet induced obesity (HFD–DIO) rat model using PDT.[26]

In this study, we aimed to develop a minimally invasive endoscopic procedure that enables non-thermal photodynamic therapy-duodenal mucosal resurfacing (PDT-DMR), the feasibility and safety of which were first evaluated in a porcine model, using a highly functional metal stent covered with a PS for treating MS.

RESULTS

Assessment of the photosensitizer retained in the PDT stent

To evaluate the dissolution of mPEG-Ce6 by light irradiation, a silicone film containing the same proportion of mPEG-Ce6 was irradiated twice with laser, and the remaining photosensitizers were measured. A silicone film containing mPEG-Ce6 retained 97%–98% of its properties even after light irradiation. Therefore, the proportion of mPEG-Ce6 that dissolved from the silicone film was very small, approximately 2%–3%, and it was confirmed that very little mPEG-Ce6 was separated from the silicone film regardless of light irradiation (supplementary material Fig. 1).

Safety and feasibility in the Yorkshire pig model

We assigned eight pigs to assess the safety and feasibility of PDT-DMR according to the survival time. In all pigs, PDT-DMR was performed safely without major adverse events, such as perforation, duodenal stricture, or bleeding. However, one case in the 7-day survival group showed distal stent migration. We failed to remove the migrated stent using biopsy forceps and sacrificed the pig. Autopsy indicated several abrasions caused by stent migration into the duodenum. Moreover, we observed a 3-cm A2-grade gastric ulcer in the stomach; however, it did not appear to be related to the stent.

Blood tests were performed to evaluate other adverse events, such as infection, bleeding, and secondary pancreatitis or cholangitis, on postoperative days 0, 1, 7, 14, 28, and 56. The results of all blood tests performed during the procedure were within reference ranges. No signs of systemic infection, pancreatitis, cholangitis, or hepatitis were observed (supplementary material Table 1). We performed follow-up radiography, endoscopy, and fluoroscopy to remove the stent and evaluate bowel perforation, obstruction, and stricture 7 days after PDT-DMR, which were not observed in any of the pigs.

We confirmed the changes in apoptotic intestinal epithelial cells after PDT-DMR using hematoxylin and eosin (H&E) and TUNEL staining. The epithelial cell layer was lost for approximately 14 days, gradually recovered, and appeared normal on day 28. Apoptotic cells were stained brown by TUNEL staining on days 7 and 14 and recovered after 28 days. The reversibility of PDT-DMR further ensured the safety of the procedure (Fig. 1).

The mean procedure time from endoscope insertion to PDT-DMR completion on the entire 15-cm length of the duodenum was 66.25 ± 11.87 min. The procedure time was reduced to 21 min upon repetition (supplementary material Table 2).

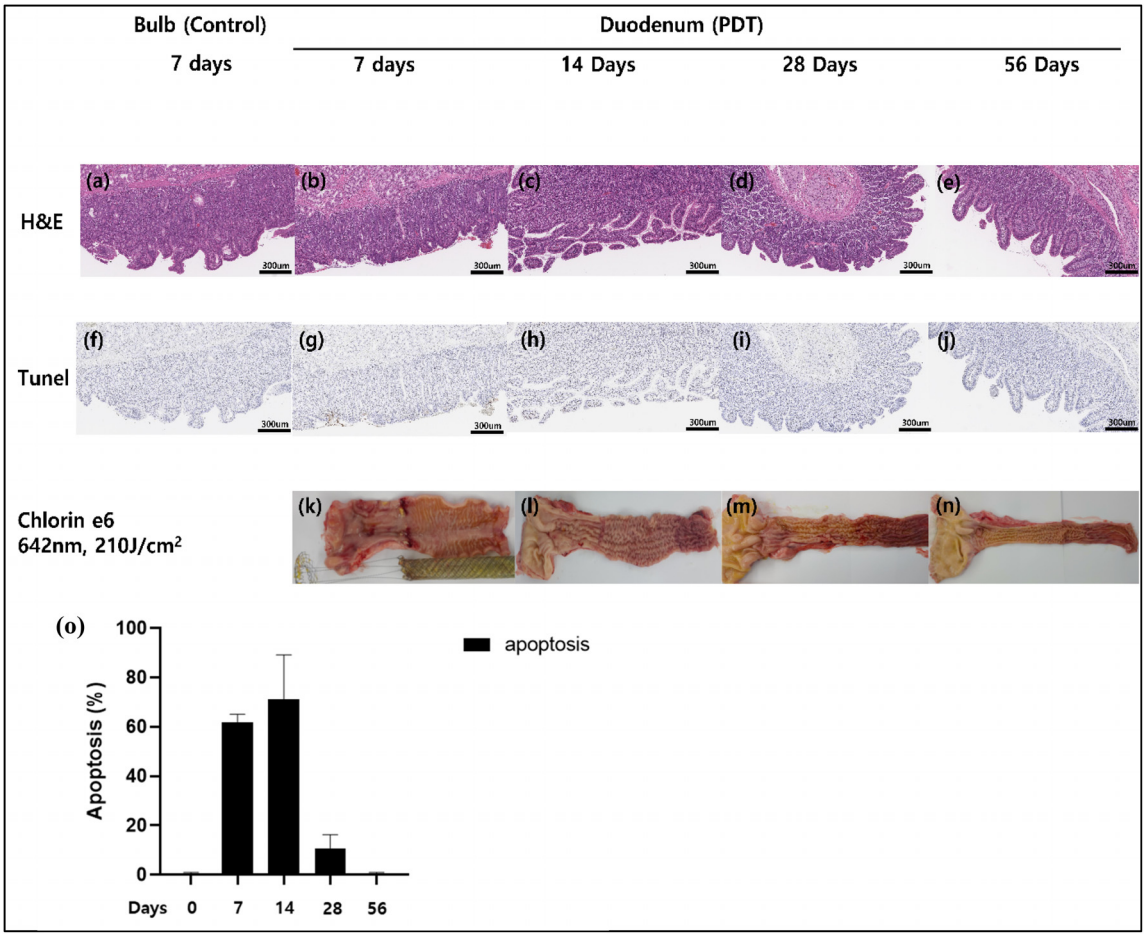

FIG. 1. Representative histology of PDT-DMR according to the duration of survival in the Yorkshire pig model (scale bar 300 μm/8.0×). (a)–(e) Representative H&E-stained images to confirm the damage or healing of the epithelium after PDT ablation depending on the time. The layer of epithelial cells is lost for approximately 14 days, gradually recovers afterward, and appears similar to normal tissues at 28 days. (f)–(j) Representative TUNEL images of PDT-operated pigs depending on the time. Brown-stained cells represent apoptotic cells via PDT-DMR. The mucosa was stained with TUNEL on days 7 and 14 and recovered after day 28. (k)–(n) Representative gross findings during the sacrifice. We observed no adverse events, such as perforation, duodenal stricture, and bleeding. Representative histology images were stained with H&E and TUNEL and captured with a 4× objective. (o) TUNEL quantification after a single PDT-DMR was performed according to the specified duration. *PDT-DMR*, photodynamic therapy-duodenal mucosal resurfacing; *H&E*, hematoxylin and eosin; *TUNEL*, terminal deoxynucleotidyl transferase dUTP nick end labeling.

Metabolic effects of PDT-DMR in the Yorkshire pig model

To determine the metabolic effects of PDT-DMR, we examined changes in the expression of incretin hormones and glucose receptors after the procedure. GIP expression was observed in the mucosal layer of the untreated bulb site regardless of the elapsed time. Conversely, GIP expression was only observed in the epithelial cells of the mucosal layer until day 14 at the PDT-DMR site, similar to that in the untreated bulb site. However, it disappeared from the epithelial cells and was only observed in the gland cells of the lamina propria on day 28. On day 56, GIP expression recovered in these gland cells. Thus, apoptosis of GIP-expressing cells was induced, which is the expected therapeutic effect of PDT-DMR (supplementary material Fig. 2). The results of the GIP expression quantification are shown in Fig. 2. GIP expression decreased significantly at the PDT-DMR site until 28 days and recovered on day 56 (Fig. 2).

GLUT1, which is typically expressed in the distal ileum and rarely observed in the duodenum, was expressed at the PDT-DMR site 14 days after the procedure. This may be attributed to the glucose metabolism activation during the recovery of the duodenal epithelium after PDT-DMR. Subsequently, expression peaked on day 28. GLUT1 expression decreased but remained low for 56 days, during the almost complete recovery of the duodenal epithelium. In the untreated bulb site, GLUT1 expression was observed on day 28, decreased afterward, and remained unchanged on day 56 (supplementary material Fig. 2). The results of the quantification of GLUT1 expression are shown in Fig. 3. GLUT1 expression increased at the PDT-DMR site and bulb on day 28, and it remained high until 56 days.

DISCUSSION

The use of thermal energy in DMR poses the risk of adverse events, such as duodenal stricture and perforation. Therefore, we developed a minimally invasive endoscopic procedure that enables non-thermal PDT for DMR. PDT-DMR was performed successfully and did not cause injury to the local tissues or systemic sequelae in a large-animal porcine model, confirming its safety and feasibility. Furthermore, we observed a decrease in duodenal GIP secretion and GLUT1 expression after PDT-DMR, consistent with the therapeutic effects expected for the treatment of patients with MS.

The PDT-DMR procedure is similar to that of the existing duodenal stenting method. Thus, the technical difficulty in its implementation is minimal, and its learning curve is expected to be short for general therapeutic endoscopists. PDT can be applied to treat a long duodenal area simultaneously using the novel PS stent. Conversely, the length of the hydrothermal DMR is insufficient to simultaneously cover the 15-cm duodenum; therefore, completing DMR is considered complex and challenging. The average procedure time for PDT-DMR was 66 min 57 s in the eight cases. The procedure time could be reduced upon repetition, and our novel PDT-DMR method is more straightforward and less complex than other DMR methods. Considering that repeated procedures are required to maintain the therapeutic effects on MS, the simplicity of PDT-DMR is a crucial

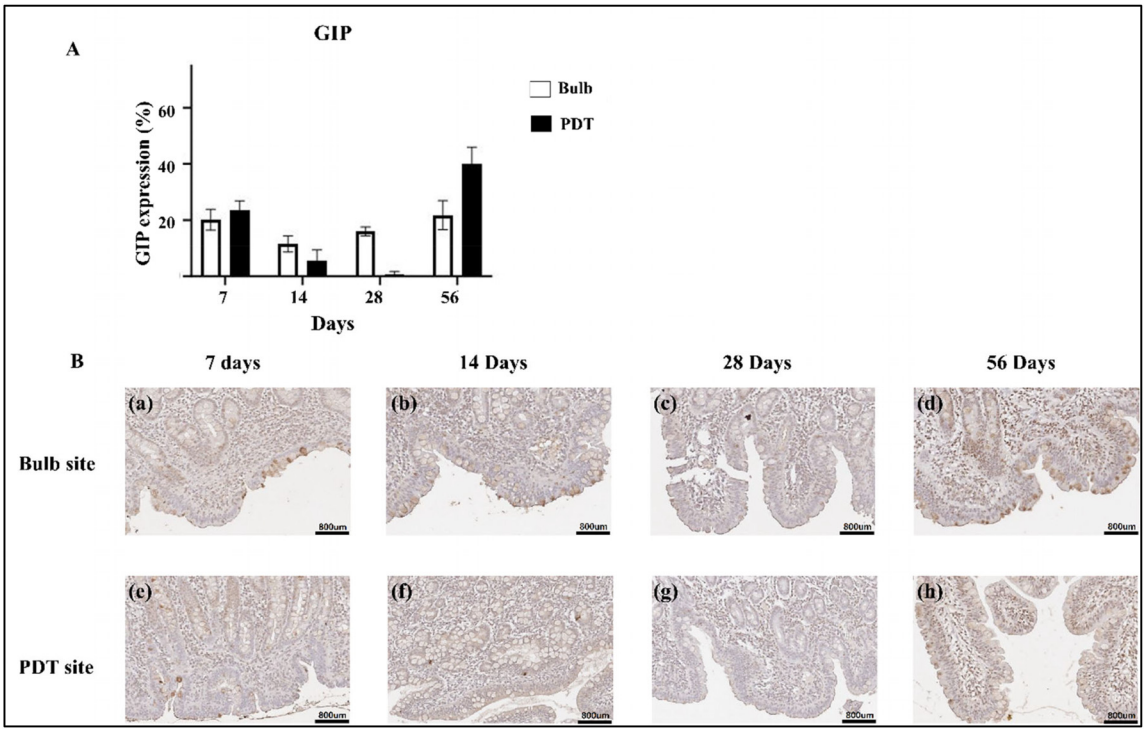

FIG. 2. PDT-DMR lowers GIP expression in the Yorkshire pig model. (A) GIP quantification after a single PDT-DMR was performed according to the specified duration. (B) (a)–(d) Representative GIP IHC-stained images of the bulb site. (e)–(h) Representative GIP IHC-stained images of the PDT-DMR site. *GIP*, gastric inhibitory polypeptide; *IHC*, immunohistochemistry.

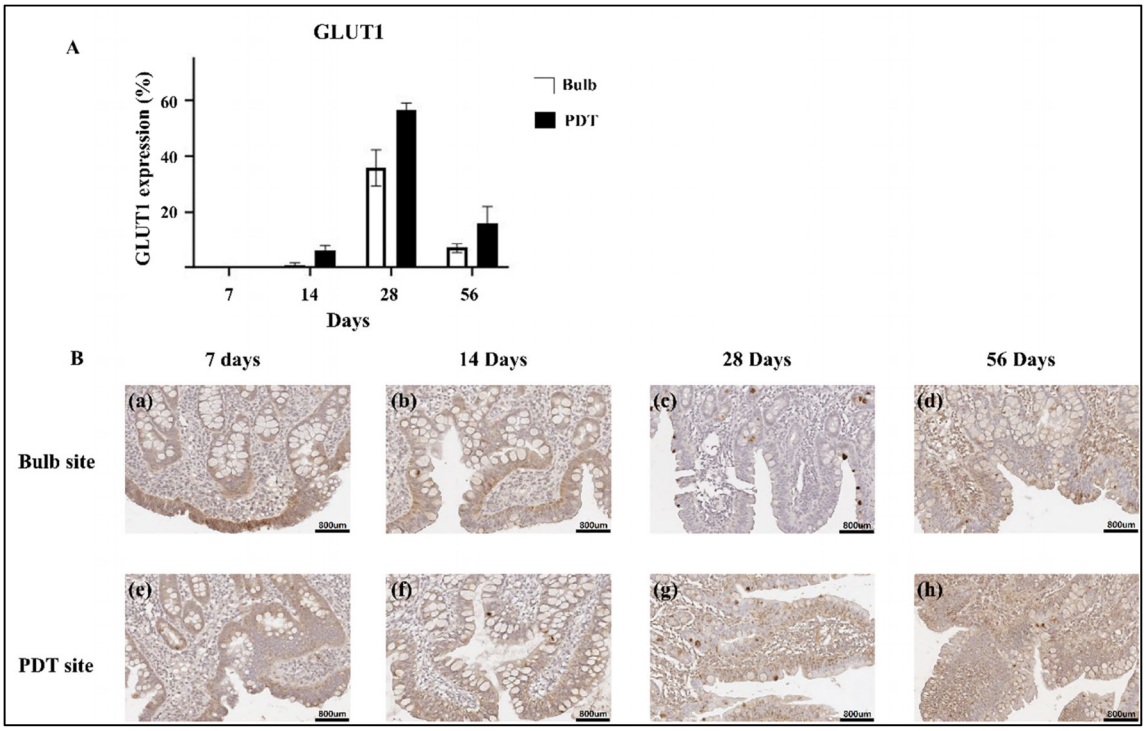

FIG. 3. GLUT1 expression is observed after PDT-DMR in the Yorkshire pig model. (A) GLUT1 quantification after a single PDT-DMR was performed according to the specified duration. (B) (a)–(d) Representative GLUT1-IHC-stained images of the bulb site. (e)–(h) Representative GLUT1-IHC-stained images of the PDT-DMR site. *GLUT1*, glucose transporter 1.

factor for practitioners to accept it as an effective treatment method. In the case of Barrett's esophagus, the PDT method using 5-aminolaevulinic acid (ALA) can be considered as treatment. ALA-PDT can be performed by simply swallowing ALA instead of using a stent.[27,28] Several studies showed that ALA-PDT is feasible in the esophagus and duodenum.[29] However, there is a lack of study on the safety and feasibility of using ALA-PDT in metabolic diseases. Thus, further clinical studies of ALA-PDT for DMR are needed. On the other hand, PDT-DMR using a duodenal stent has the advantages of effectively targeting the duodenum and preventing duodenal stricture after the procedure compared to ALA-PDT.

Notably, as a non-thermal ablation method that induces ROS to trigger apoptosis in superficial mucosal epithelia, PDT-DMR can help prevent unwanted injury to the deep layer. The PS itself cannot penetrate mucosal cells but instead relies on diffusion of singlet oxygen from the stent surface into the cells. As the activated ROS have a short half-life ($<0.04\,\mu s$) and diffusion distance ($<0.02\,\mu m$), we designed the duodenal stent to be extremely adjacent to the mucosal wall. Additionally, several studies have already confirmed the apoptosis effect of PDT-DMR *in vitro*.[30–32] By placing a film containing methylene blue (MB) or mPEG-Ce6 directly on the cells and irradiating them with a laser, these studies experimentally confirmed that cell apoptosis actually occurred. We observed no fatal adverse effects, such as perforation and stricture without mucosal lifting. To protect against distal migration, we designed a funnel-shaped anti-migration structure and a second middle wire part as a buffer structure against peristalsis. However, stent migration occurred in one of the eight pigs. Therefore, a complementary study is required to explore strategies for preventing distal migration. The histological analysis shows that PDT-DMR is a reversible and safe procedure that can overcome the disadvantages of surgery and simultaneously achieve similar treatment effects.

Hormones secreted from the duodenum alter metabolism and are closely related to the induction of obesity and insulin resistance. Insulin resistance is a key risk factor for MS and plays a critical role in the pathological progression and decompensation of multiple organ systems in T2DM. Several hormones are involved in glycemic control, and incretin hormones are associated with diabetes and obesity. Incretins are a group of metabolic hormones that decrease blood glucose levels, consisting of GIP secreted by duodenal K-cells and glucagon-like peptide-1 secreted by the L-cells of the lower intestine. GIP promotes insulin secretion in healthy individuals. Conversely, in patients with obesity and T2DM, prolonged exposure of GIP receptor-expressing tissues to GIP can produce severe downregulation, leading to desensitization of GIP receptors and impaired GIP sensitivity of the tissue.[33,34] Moreover, its infusion impairs postprandial plasma lipids and increases postprandial glycemia and glucagon concentration in patients with T2DM.[35] Consequently, increased GIP expression can aggravate MS in patients with obesity.[36,37] Several studies have confirmed GIP suppression following endoscopic DMR for MS treatment; however, adverse events are inevitable because of thermal energy.[17,38,39] Therefore, we focused on PDT-DMR to avoid affecting the deep mucosal layers. Na *et al.* have confirmed the potential for

treating obesity with T2DM by inhibiting GIP release from the K-cells using endoscopic PDT in an *in vivo* model.[40]

IHC staining was performed to verify the effects of incretin hormone regulation in a Yorkshire pig model. The PDT-DMR method suppressed GIP expression and activated GLUT1 expression in the small intestine. GLUT1 was not detected in the small intestines of non-diabetic animals.[41] GLUT1 is expressed in the apical and basolateral membranes of the small intestine after RYGB, resulting in increased serum glucose excretion in the gut lumen.[25] Therefore, GLUT1 expression may help reduce hyperglycemia. However, further mechanistic and clinical studies of GLUT1 expression using PDT-DMR are crucial. Nonetheless, our findings suggest that PDT-DMR can reduce fat accumulation, glucagon levels, and body weight by suppressing GIP secretion and GLUT 1 expression in the mucosa of the duodenum.

The expression of GIP, which was initially reduced by PDT, increased in the gland cells of the lamina propria as the mucosa recovered, confirming the restoration of K-cells in the gland cells. The time required for the GIP receptor to be upregulated again and for the insulinotropic effect of GIP to be fully restored remains unclear. In the case of GLUT1, the expression level peaked on day 28 at the bulb and PDT site, decreasing by day 56. However, some expression was still observed on day 56. GLUT1 expression was also induced in the bulb without PDT, suggesting potential effectiveness in lowering blood sugar by increasing serum glucose excretion in the gut lumen. Therefore, repeat procedures may be necessary, but we can expect that the proportion of K-cells and L-cells may change during mucosal regeneration, as indicated by our mouse study. Notably, hydrothermal DMR studies also showed mucosal regeneration by 6 weeks after the procedure; however, in human models, the therapeutic effects were maintained through 6 months of follow-up.[11,42] Unlike bariatric surgery, which irreversibly changes the anatomical structure, this procedure carries the advantage of being repeatable without changing the anatomical structure. The results observed in the Otsuka Long-Evans Tokushima (OLETF) male rat HFD–DIO model were also validated in the porcine model.[26] Although it was not feasible to create a diabetes model in the Yorkshire pig, we theoretically demonstrated the effectiveness of PDT-DMR in treating metabolic diseases in obese patients.

The strength of this novel study is that it demonstrated the feasibility and safety of the non-thermal ablation method for DMR in a large-animal porcine model. Despite some PDT-related studies in small animal models, such as rats, further research is required to confirm feasibility in large-animal models with organ structures similar to those of humans. However, this study had some limitations. First, the number of pigs was insufficient to derive the final results. Second, Yorkshire pigs are unsuitable for demonstrating the effects of PDT-DMR on obesity, owing to their rapid growth rate. Third, we could not confirm the therapeutic effects of diabetes in the Yorkshire pigs because it was impossible to create a diabetic pig model. Fourth, we did not examine the selectivity of PDT. Unlike cancer treatment, which targets diseased cells specifically, the goal of PDT-DMR is to induce apoptosis in an unspecified number of normally distributed K-cells. Thus, unlike PDT for cancer treatment, the therapeutic effect can be achieved by causing damage to as many cells as possible in the corresponding segment through the stent. Finally, experiments with species most similar to the human body are critical for determining feasibility before human application, even if the differences in anatomy cannot be overcome. Therefore, researchers should consider various aspects to ensure safety before applying PDT-DMR to humans. To overcome these limitations, further studies employing alternative animal models, such as minipigs and dogs, should be conducted.

CONCLUSIONS

PDT-DMR is a safe and effective EBMT method applicable to the human body. Furthermore, the procedure is similar to the duodenal stenting method; therefore, the expected time required to reach the learning curve is short. We observed reduced GIP expression and increased GLUT-1 expression, demonstrating the therapeutic effects of PDT-DMR. Therefore, this PDT-DMR procedure can serve as a bridge between lifestyle modifications, drug treatment, and surgical treatment in the existing spectrum of metabolic disease treatments.

METHODS

Developmental study

Stent development

We developed a novel tool—specifically, a highly functional metal stent covered with PS for PDT-DMR—tailored to work on the unique anatomy of the human duodenum. The stent comprised three parts [Fig. 4(a)]: (i) a funnel-shaped anti-migration structure designed to prevent distal migration and enable safe removal when required; (ii) a 10-cm middle wire, which was left blank with only four wires to prevent blockage of the ampulla of Vater while preventing secondary cholangitis or pancreatitis; and (iii) a PS membrane as the primary body part with a 15-cm silicon cover, which came into contact with the duodenum from the second to third portions where the mucosal ablation treatment occurred. A lasso was attached to the proximal end of the stent body to enable safe removal without damaging the mucous membrane using biopsy forceps [supplementary material Fig. 3(a)]. Tungsten plated markers were placed at the proximal, middle, and distal parts of the stent to identify the location of the stent when capturing radiographs. The PS membrane comprised three layers: an outer stent, a silicon cover containing a PS, and an inner stent. The irradiation device was developed to position the light source at the center of the curved duodenal lumen such that it could access the silicon cover, including the PS stent, evenly and with equal energy [supplementary material Fig. 3(a)]. The irradiation stent was designed to be deployed and recaptured freely inside the PS stent and can accommodate a laser diffuser that acts as a light source [supplementary material Fig. 3(b)].

Photosensitizer development

Recently, MB has been developed for the treatment of metabolic diseases and cancer therapy, with its therapeutic effects validated in a pig model.[30] MB is an inexpensive, nontoxic dye that is widely used in medical treatment as it shows strong absorption of broadband red light (550–700 nm) and strong photodynamic efficiency.[43] With the ultimate goal of application to the human body, PS available in Korea was first selected and verified. In this process, MB was also considered as an option. However, Chlorin e6 (Ce6) and its derivative forms exhibit superior photo-responsiveness due to higher triplet energy (Ce6: 269 vs MB: 109.2 kJ/mol) and singlet oxygen yield (Ce6: 0.7 vs MB: 0.5Φ) compared to MB. Consequently, Ce6 is anticipated to be more advantageous in inducing cell death, cell stimulation, and reducing ghrelin secretion.[43–45] We specifically selected Ce6 as it is characterized by a

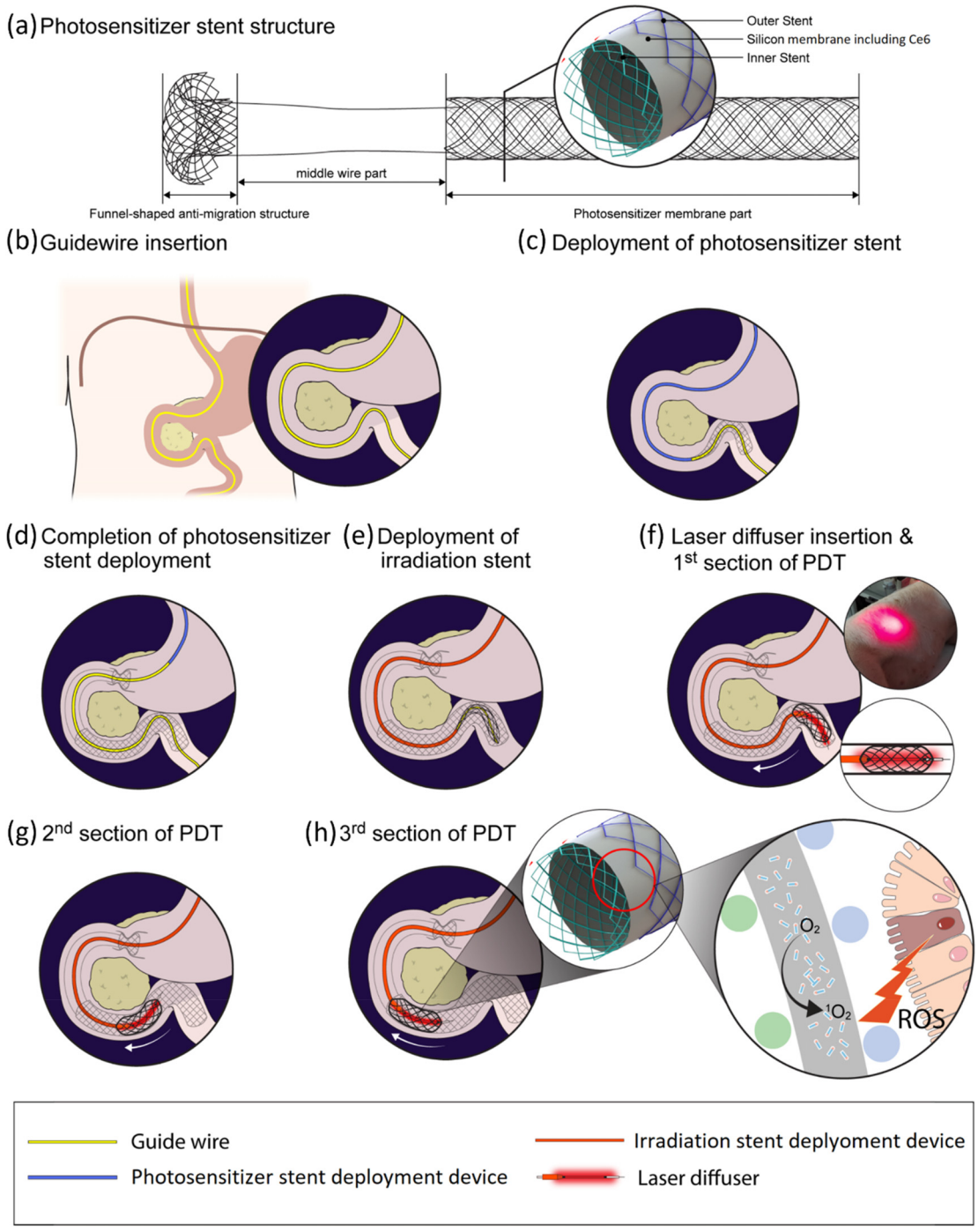

FIG. 4. Schematic diagram of the photodynamic therapy-based duodenal mucosal resurfacing. (a) Photosensitizer stent structure. (b) Guidewire insertion. (c) Deployment of photosensitizer stent. (d) Completion of photosensitizer stent deployment. (e) Deployment of irradiation stent. (f) Laser diffuser insertion and 1st section of PDT. (g) 2nd section of PDT. (h) 3rd section of PDT.

high quantum yield, producing more ROS per photon than first-generation photosensitizers. This increased effectiveness against cell damage is accompanied by a shorter half-life in the body, leading to rapid elimination and reduced risk of long-term side effects.[46]

Free Ce6 for anticancer treatment exhibits a strong hydrophobic feature, hindering rapid elimination from the human body. Conversely, polymer-bound Ce6, with a tenfold larger molecular weight than free Ce6, ensures consistent coating, minimal absorption

into the body, enhanced retention on the device membrane, and repeatable PDT during the indwell time.[47,48] We evaluated retained mPEG-Ce6 in the PDT stent based on the presence or absence of light irradiation. The process involved dispensing 0.1 ml of PEG-5K Ce6 silicone solution onto glass, drying at 150 °C for 3 h, obtaining a film, immersing it in 0.1 M phosphate buffer solution (containing 0.1% surfactant), irradiating with laser, and storing in a constant temperature water bath at 37 °C and 50 rpm to induce dissolution. Four experimental groups were designed, including (i) laser irradiation (5 J/cm^2) on day 0 of the experiment, (ii) laser irradiation (33 J/cm^2) on day 0 of the experiment, (iii) laser irradiation (5 J/cm^2) on days 0 and 1 of the experiment, and (iv) laser irradiation (33 J/cm^2) on days 0 and 1 of the experiment. After laser irradiation, all groups were dissolved for 10 days, and Ce6 in the supernatant was quantified daily based on absorbance using a UV-Vis spectrophotometer.

Our methodology was informed by the study of Kim *et al.*, who demonstrated the cytotoxicity and phototoxicity of mPEG-Ce6 using mouse connective tissue cells and human stomach cells.[31] The singlet oxygen generation efficacy of mPEG-Ce6 was measured using SOSG and DMA. SOSG (10 μM) or DMA (20 $\times$ 10^{-3} mM) was diluted in de-ionized water, and mPEG-Ce6 was dissolved in this solution at a concentration of 10 μg per 2 ml of Ce6. It was quantified with UV spectra. A fragment of the photosensitizer stent was placed in an SOSG or DMA solution to measure the ROS generation of the Ce6-embedded photosensitizer stent. Ce6 was irradiated with a 670 nm red light (Fiber Coupled Laser Modules, LaserLab®, Seoul, Korea) (total 10 J/cm^2; 20 mW/cm^2, 20 s, 25 measurements). The fluorescence intensity of SOSG was detected using fluorescence spectroscopy (RF-5301, Shimadzu, Kyoto, Japan) (Ex/Em = 504 nm/525 nm), and the fluorescence intensity of DMA was determined using radio frequency spectrum analysis (Ex/Em = 375 nm/436 nm).[31]

To synthesize mPEG-Ce6, we initially proceed with the synthesis of Ce6-NHS. Ce6 (0.3 g), 1,3-dicyclohexylcarbodiimide (DCC, 0.12 g), and N-hydroxy succinimide (NHS, 0.70 g) were dissolved in 10 ml of anhydrous methylene chloride (MC) and stirred at room temperature (RT) for 4 h. Simultaneously, mPEG-amine (5KDa, 1.68 g) was completely dissolved in 40 ml of anhydrous MC. After the Ce6-NHS synthesis, the unreacted Ce6 aggregates were filtered with a 0.45-μm PTFE syringe filter. The filtered Ce6-NHS was dropped into the mPEG-amine solution and stirred at RT for 24 h. The mixture was precipitated in excessive ice-cold ether, centrifuged at 3500 rpm for 6 min, then completely dried in a vacuum oven. The unreacted Ce6 and mPEG-amine were purified via Sephadex LH-20 organic solvent size-exclusion chromatography, using methanol as eluent. The mPEG-Ce6 fraction was evaporated to remove the solvent and lyophilized for 3 days. The final product was confirmed through 1H-nuclear magnetic resonance spectroscopy and Fourier transform infrared spectroscopy.[31]

To prepare the Ce6-embedded photosensitizer stent, a 20 ml mPEG-Ce6 silicone coating solution composed of silicone, xylene, and volatile solvent was used. The dip coating technique was employed for the fabrication of the Ce6-embedded photosensitizer stent. The photosensitizer membrane part was dipped in the Ce6-silicone solution for 20 s and slowly withdrawn. It was immediately dried in an oven at 150 °C for 2 h and then air-dried for 30 min at RT (20–25 °C).[31]

Procedural development

PDT-DMR was designed to trigger endocrine cell apoptosis of the duodenal mucosal wall while minimizing the risk of adverse events, such as injury of the deep layer of the duodenal wall and intestinal stricture. Through developmental studies using porcine models, we confirmed the appropriate concentration of PS and the optimal laser energy to induce apoptosis of the mucosal walls. During procedural development, duodenal wall perforation occurred at an energy of 240 J/cm. Safety was confirmed by setting the laser output to 1.5 W and irradiating energy to a 5 cm length of PDT stent for 700 s. Thus, the energy of the laser was fixed at 210 J/cm. The Ce6 laser wavelength was set to 662 nm using an endoscopic illumination laser system (LAKHTA-MILON, Russia).[40] The PDT-DMR procedure was established through developmental protocols [Figs. 4(b)–4(h)]. First, the PS stent was tracked over a 0.035-in. guidewire and placed in the proximal duodenum distal to the papilla. Second, the irradiation device was advanced into the PS stent. Third, an irradiation device was deployed. Fourth, a 5-cm laser diffuser providing the light energy necessary for ROS generation was placed in a transparent tube inside the irradiation device. Fifth, irradiation was performed at the most distal end of the third PS membrane, and the diffuser was sequentially pulled out to the next proximal part upon completion, circumferentially ablating 15-cm of duodenal tissues over three times during a single endoscopic session. Last, after laser diffuser removal, we recaptured the irradiation device. PS stents were placed for 7 days to prevent duodenal stricture formation after PDT-DMR (supplementary material video 1).

Feasibility and safety study

The feasibility and safety of the PDT-DMR procedures were assessed in Yorkshire pigs, which are similar to humans regarding luminal diameter, mucosal thickness of the intestines, and endoscopic access to the duodenum. Yorkshire swine with a body weight ranging from 24.6 to 39.4 kg (n = 8; mean weight, 32.8 kg) were fasted for 24 h before the procedure. The animals received care according to the guidelines of the Laboratory Animal Care Committee of the Yonsei University Health System (approval number: 2020–0255). PDT-DMR was performed under general anesthesia, induced by an initial intramuscular injection of ketamine hydrochloride (22 mg/kg) and atropine (0.005 mg/kg). Sodium pentobarbital (10 mg/kg) was administered via the marginal ear vein. The pigs were placed in a supine position, intubated with a soft-cuff 6.0-Fr endotracheal tube, and received isoflurane (2.0%) and oxygen via a ventilator. We monitored a tidal volume of 10 ml/kg and a respiratory rate of 16 breaths per minute. Anesthesia was restored by discontinuing isoflurane and maintaining the pigs on a ventilator with oxygen until adequate spontaneous ventilation was restored.

We assigned two Yorkshire pigs to each of the 7-, 14-, 28-, and 56-day survival groups, based on the survival duration after a single PDT-DMR procedure. In all pigs, the stent was maintained until day 7 after PDT-DMR to prevent duodenal stricture, and they were sacrificed on postoperative days 7, 14, 28, and 56. Untreated tissues of the duodenal bulb and PDT-DMR-treated tissues of the second to third duodenum were obtained after sacrifice and stained with H&E and terminal deoxynucleotidyl transferase dUTP nick end labeling (TUNEL) to analyze the PDT-DMR-mediated changes in the mucosal and submucosal layers.

Blood samples were obtained from the ear veins immediately before and 24 h after the procedure and at postoperative days 7, 14, 28, and 56 to evaluate hemoglobin, leukocytes, platelets, albumin, aspartate aminotransferase, alanine aminotransferase, C-reactive protein,

blood urea nitrogen, and creatinine levels. Postprocedural perforation and stent migration were assessed radiographically. The body weights and temperatures were measured weekly.

Metabolic effects of PDT-DMR

The duodenum tissues were analyzed by immunohistochemistry (IHC) to evaluate metabolic change after PDT-DMR. To compare the GIP and GLUT1 expression levels after PDT-DMR, we performed IHC staining on untreated tissues of the duodenal bulb and PDT-DMR-treated tissues of the second and third parts of the duodenum. For IHC, formalin fixed and paraffin embedded duodenum tissue (5-μm thick sections) were stained. Sections were incubated in 0.3% H_2O_2-MeOH for 20 min and pre-incubated in 2.5% normal horse serum to reduce nonspecific staining. Tissue sections were incubated overnight in a humid chamber at 4 °C with the following antibodies: rabbit polyclonal to GIP (1:1000, Lsbio, Washington, USA; LS-B6690) and rabbit polyclonal to GLUT-1 (1:100, Abcam, Cambridge, UK; ab14683) diluted in PBS (supplementary material Table 3). After several rinses with PBS, slides were stained with DAB (Vector labs) and examined under a light microscope equipped with an Olympus digital camera.

The IHC was divided into a grid and some parts were magnified. To quantify GIP and GLUT1 expression, the expressed GIP and GLUT1 were counted and the percentage ratio was expressed graphically.

Statistical analysis

The primary end point was the technical feasibility and safety of PDT-DMR using a PS stent, and the secondary end point was the metabolic effects. We reported summary data as means and standard estimated measures using IBM SPSS Statistics (version 26.0; SPSS, Chicago, IL, USA). For quantification of the immunohistochemical results, cells stained with specific reagents were counted in a portion of the magnified section and expressed as a percentage. We visualized the quantification data via a bar graph using GraphPad Prism (version 10.2.2.; Prism, Boston, USA).

SUPPLEMENTARY MATERIAL

See the supplementary material for details:

Supplementary Figure 1:

- Figure (.pdf)
- Residual amount of mPEG-Ce6 in silicone film after laser irradiation.
- Red arrow: Laser irradiation point, 1×: Laser irradiation at 0 day, 2×: Laser irradiation at 0 day and 1 day

Supplementary Figure 2:

- Figure (.pdf)
- Representative GIP, GLUT1 IHC staining

PDT-DMRPDT–DMR lowers GIP expression in the Yorkshire pig model. GIP IHC staining (antibody: Lsbio, LS-C204195) after a single PDT-DMR was performed according to the specified duration. (a)–(d) Representative GIP IHC-stained images on the bulb site. GIP expression is observed in the mucosal layer regardless of the day. (e)–(h) Representative GIP IHC-stained images on the PDT-DMR site. (g) GIP expression disappeared in the epithelial cells of the mucosal layer on day 28. (h) GIP expression recovered in the gland cells of the lamina propria on day 56. *GIP*, gastric inhibitory polypeptide; *IHC*, immunohistochemistry. GLUT1 expression is observed after PDT-DMRPDT-DMR in the Yorkshire pig model. GLUT1-IHC staining (antibody: Abcam, ab14683) after a single PDT-DMRPDT-DMR was performed according to the specified duration. (i)–(l) Representative GLUT1-IHC stained images of the bulb site. (j) GLUT1 expression is observed from 14 days after PDT-DMRPDT-DMR. (k) GLUT1 expression peaks on day 28. (l) GLUT1 expression persists on day 56. (m)–(p) Representative GLUT1-IHC stained images of the PDT-DMRPDT-DMR site. (n) GLUT1 expression is observed from 14 days after PDT-DMRPDT-DMR. (o) GLUT1 expression peaks on day 28. (p) GLUT1 expression persists on day 56. *GLUT1*, glucose transporter 1.

Supplementary Figure 3:

- Figure (.pdf)
- The structure of novel tools.
- (a). The PS stent consists of three parts. (b). The irradiation stent is designed to be deployed and recaptured freely and can accommodate a laser diffuser, which acts as a light source. *PS*, photosensitizer.

Supplementary video 1:

- Video (.MP4)
- PDT-DMRPDT-DMR video
- This supplementary video material is uploaded on Zenodo (Ref. 49).

Supplementary Table 1:

- Table (.pdf)
- Blood chemistry and post-procedure blood cell counts
- The results of blood test are organized over time.

Supplementary Table 2:

- Table (.pdf)
- Photodynamic therapy-duodenal mucosal resurfacing procedure time
- We measured the procedure time by recording the endoscopy start and end times. The procedure time was reduced by 21 min upon repetition.

Supplementary Table 3:

- Table (.pdf)
- List of reagents used in IHC staining
- The reagents we used for immunohistochemistry staining are summarized.

ACKNOWLEDGMENTS

This work was supported by the Korea Medical Device Development Fund grant funded by the Korean government (the Ministry of Science and ICT; the Ministry of Trade, Industry and Energy; the Ministry of Health & Welfare; the Ministry of Food and Drug Safety) (Project Nos. 1711137983 and KMDF_PR_20200901_0036).

AUTHOR DECLARATIONS

Conflict of Interest

The authors have no conflicts to disclose.

Ethics Approval

Ethics approval for experiments reported in the submitted manuscript on animal or human subjects was granted. The animals received care according to the guidelines of the Laboratory Animal Care Committee of the Yonsei University Health System (Approval number: 2020-0255).

Author Contributions

Chan Su Park: Visualization (supporting); Writing – original draft (lead); Writing – review & editing (equal). **Hyun Jin Park:** Data curation (equal); Visualization (supporting). **Ji Hoon Park:** Writing – original draft (supporting). **Jin Hee Lee:** Data curation (equal). **Hyun Jung Kee:** Data curation (equal). **Jung-Hoon Park:** Conceptualization (equal). **Jung Hyun Jo:** Writing – review & editing (supporting). **Hee Seung Lee:** Writing – review & editing (supporting). **Cheol Ryong Ku:** Conceptualization (equal). **Jeong Youp Park:** Writing – review & editing (supporting). **Seungmin Bang:** Writing – review & editing (supporting). **Jung Min Song:** Conceptualization (equal). **Kun Na:** Conceptualization (equal). **Sung Kwon Kang:** Conceptualization (equal). **Hwoon-Yong Jung:** Conceptualization (equal). **Moon Jae Chung:** Conceptualization (equal); Data curation (equal); Funding acquisition (equal); Methodology (equal); Supervision (lead); Validation (lead); Visualization (equal); Writing – original draft (supporting); Writing – review & editing (supporting).

DATA AVAILABILITY

The data that support the findings of this study are available from the corresponding author upon reasonable request.

REFERENCES

[1]E. Kassi, P. Pervanidou, G. Kaltsas, and G. Chrousos, BMC Med. **9**, 48 (2011).
[2]S. S. Daskalopoulou, D. P. Mikhailidis, and M. Elisaf, Angiology **55**(6), 589–612 (2004).
[3]E. Standl, K. Khunti, T. B. Hansen, and O. Schnell, Eur. J. Prev. Cardiol. **26**(2), 7–14 (2019).
[4]S. M. Grundy, J. I. Cleeman, C. N. Merz, H. B. Brewer, Jr., L. T. Clark, D. B. Hunninghake, R. C. Pasternak, S. C. Smith, Jr., N. J. Stone, and for the Coordinating Committee of the National Cholesterol Education Program and Endorsed by the National Heart, Lung, and Blood Institute, American College of Cardiology Foundation, and American Heart Association, Circulation **110**(2), 227–239 (2004).
[5]L. M. Carlsson, M. Peltonen, S. Ahlin, A. Anveden, C. Bouchard, B. Carlsson, P. Jacobson, H. Lonroth, C. Maglio, I. Naslund, C. Pirazzi, S. Romeo, K. Sjoholm, E. Sjostrom, H. Wedel, P. A. Svensson, and L. Sjostrom, N. Engl. J. Med. **367**(8), 695–704 (2012).
[6]P. R. Schauer, S. R. Kashyap, K. Wolski, S. A. Brethauer, J. P. Kirwan, C. E. Pothier, S. Thomas, B. Abood, S. E. Nissen, and D. L. Bhatt, N. Engl. J. Med. **366**(17), 1567–1576 (2012).
[7]S. Kahan and A. Williams, Ann. Intern. Med. **174**(9), JC101 (2021).
[8]E. G. H. de Moura, A. M. Ponte-Neto, A. Tsakmaki, V. D. Aiello, G. A. Bewick, and V. O. Brunaldi, Endosc. Int. Open **7**(5), E685–E690 (2019).
[9]D. Raddatz, Digestion **100**(3), 147–151 (2019).
[10]P. Jirapinyo and C. C. Thompson, Clin. Gastroenterol. Hepatol. **15**(5), 619–630 (2017).
[11]R. J. Haidry, A. C. van Baar, M. P. Galvao Neto, H. Rajagopalan, J. Caplan, P. S. Levin, J. J. Bergman, L. Rodriguez, J. Deviere, and C. C. Thompson, Gastrointestm Endosc. **90**(4), 673–681 (2019).
[12]A. Hadefi, V. Huberty, A. Lemmers, M. Arvanitakis, D. Maggs, G. Costamagna, and J. Deviere, Dig. Dis. **36**(4), 322–324 (2018).
[13]H. Rajagopalan, A. D. Cherrington, C. C. Thompson, L. M. Kaplan, F. Rubino, G. Mingrone, P. Becerra, P. Rodriguez, P. Vignolo, J. Caplan, L. Rodriguez, and M. P. Galvao Neto, Diabetes Care **39**(12), 2254–2261 (2016).
[14]A. C. G. van Baar, F. Holleman, L. Crenier, R. Haidry, C. Magee, D. Hopkins, L. Rodriguez Grunert, M. Galvao Neto, P. Vignolo, B. Hayee, A. Mertens, R. Bisschops, J. Tijssen, M. Nieuwdorp, C. Guidone, G. Costamagna, J. Deviere, and J. Bergman, Gut **69**(2), 295–303 (2020).
[15]A. C. G. van Baar, J. Deviere, D. Hopkins, L. Crenier, F. Holleman, M. P. Galvao Neto, P. Becerra, P. Vignolo, L. Rodriguez Grunert, G. Mingrone, G. Costamagna, M. Nieuwdorp, C. Guidone, R. J. Haidry, B. Hayee, C. Magee, J. C. Lopez-Talavera, K. White, V. Bhambhani, E. Cozzi, H. Rajagopalan, and J. J. G. H. M. Bergman, J. Diabetes Res. Clin. Pract. **184**, 109194 (2022).
[16]G. Mingrone, A. C. van Baar, J. Deviere, D. Hopkins, E. Moura, C. Cercato, H. Rajagopalan, J. C. Lopez-Talavera, K. White, V. Bhambhani, G. Costamagna, R. Haidry, E. Grecco, M. Galvao Neto, G. Aithal, A. Repici, B. Hayee, A. Haji, A. J. Morris, R. Bisschops, M. D. Chouhan, N. S. Sakai, D. L. Bhatt, A. J. Sanyal, J. J. G. H. M. Bergman, and Investigators of the REVITA-2 Study, Gut **71**(2), 254–264 (2022).
[17]A. C. G. van Baar, S. Meiring, F. Holleman, D. Hopkins, G. Mingrone, J. Deviere, M. Nieuwdorp, and J. Bergman, Gut **70**(11), 2196–2204 (2021).
[18]R. R. Allison and K. Moghissi, Clin. Endosc. **46**(1), 24–29 (2013).
[19]R. Muller-Velten, S. Michels, U. Schmidt-Erfurth, and H. Laqua, Ophthalmologe **100**(5), 384–390 (2003).
[20]U. Schmidt-Erfurth and H. Laqua, Ophthalmologe **98**(2), 216–219; quiz 230 (2001).
[21]S. Gremlich, A. Porret, E. H. Hani, D. Cherif, N. Vionnet, P. Froguel, and B. Thorens, Diabetes **44**(10), 1202–1208 (1995).
[22]H. C. Fehmann, R. Goke, and B. Goke, Endocr. Rev. **16**(3), 390–410 (1995).
[23]P. R. Schauer, D. L. Bhatt, J. P. Kirwan, K. Wolski, S. A. Brethauer, S. D. Navaneethan, A. Aminian, C. E. Pothier, E. S. Kim, S. E. Nissen, S. R. Kashyap, and S. Investigators, N. Engl. J. Med. **370**(21), 2002–2013 (2014).
[24]W. J. Pories, M. S. Swanson, K. G. MacDonald, S. B. Long, P. G. Morris, B. M. Brown, H. A. Barakat, R. A. deRamon, G. Israel, J. M. Dolezal *et al.*, Ann. Surg. **222**(3), 339–352 (1995).
[25]I. G. Kwon, C. W. Kang, J. P. Park, J. H. Oh, E. K. Wang, T. Y. Kim, J. S. Sung, N. Park, Y. J. Lee, H. J. Sung, E. J. Lee, W. J. Hyung, S. J. Shin, S. H. Noh, M. Yun, W. J. Kang, A. Cho, and C. R. Ku, Gut **70**(10), 1847–1856 (2021).
[26]S. Lee, M. J. Chung, M. Ahn, H. J. Park, E. K. Wang, T. Guon, H. J. Kee, C. R. Ku, and K. Na, Biomaterials **302**, 122336 (2023).
[27]J. M. Dunn, G. D. Mackenzie, M. R. Banks, C. A. Mosse, R. Haidry, S. Green, S. Thorpe, M. Rodriguez-Justo, A. Winstanley, M. R. Novelli, S. G. Bown, and L. B. Lovat, Lasers Med, Sci **28**(3), 707–715 (2013).
[28]P. Hinnen, F. W. de Rooij, W. C. Hop, A. Edixhoven, H. van Dekken, J. H. Wilson, and P. D. Siersema, J. Photochem. Photobiol., B **68**(1), 8–14 (2002).
[29]J. Regula, A. J. MacRobert, A. Gorchein, G. A. Buonaccorsi, S. M. Thorpe, G. M. Spencer, A. R. Hatfield, and S. G. Bown, Gut **36**(1), 67–75 (1995).
[30]S. Lee, J. W. Kim, J. Park, H. K. Na, D. H. Kim, J. H. Noh, D. S. Ryu, J. M. Park, J. H. Park, H. Y. Jung, and K. Na, ACS Appl Mater Interfaces **14**(15), 17621–17630 (2022).
[31]J. W. Kim, S. Lee, D. S. Ryu, J. Park, H. Lee, H. K. Na, J. H. Noh, D. H. Kim, J. H. Park, H. Y. Jung, and K. Na, Biomaterials **299**, 122159 (2023).
[32]D. S. Ryu, J. W. Kim, H. Lee, S. J. Eo, S. H. Kim, J. H. Noh, Y. Kim, S. Kang, K. Na, J. H. Park, and D. H. Kim, ACS Biomater. Sci. Eng. **10**(3), 1869–1879 (2024).
[33]K. H. Lok, N. J. Wareham, R. S. Nair, C. W. How, and L. H. Chuah, Pharmacol. Res. **180**, 106237 (2022).
[34]S. Del Prato, B. Gallwitz, J. J. Holst, and J. J. Meier, Obes. Rev. **23**(2), e13372 (2022).
[35]N. C. Bergmann, L. S. Gasbjerg, S. M. Heimburger, L. S. L. Krogh, F. Dela, B. Hartmann, J. J. Holst, L. Jessen, M. B. Christensen, T. Vilsboll, A. Lund, and F. K. Knop, Diabetes Care **43**(3), 588–596 (2020).
[36]J. Michalowska, E. Miller-Kasprzak, and P. Bogdanski, Nutrients **13**(2), 351 (2021).

[37]M. A. Nauck and J. J. Meier, Diabetes Obes. Metab. **20**(1), 5–21 (2018).
[38]A. Hadefi, M. Arvanitakis, V. Huberty, and J. Deviere, United Eur. Gastroenterol. J. **8**(6), 685–694 (2020).
[39]G. H. P. de Oliveira, D. T. H. de Moura, M. P. Funari, T. R. McCarty, I. B. Ribeiro, W. M. Bernardo, V. M. T. Sagae, J. R. Freitas, Jr., G. M. V. Souza, and E. G. H. de Moura, Obes. Surg. **31**(3), 1304–1312 (2021).
[40]S. Lee and K. Na, Biomaterials **246**, 119977 (2020).
[41]S. Boyer, P. A. Sharp, E. S. Debnam, S. A. Baldwin, and S. K. Srai, FEBS Lett. **396**(2–3), 218–222 (1996).
[42]A. C. G. van Baar, S. Meiring, P. Smeele, T. Vriend, F. Holleman, M. Barlag, N. Mostafavi, J. G. P. Tijssen, M. R. Soeters, M. Nieuwdorp, and J. Bergman, Gastrointest. Endosc. **94**(1), 111–120 e113 (2021).
[43]M. Wagner, E. R. Suarez, T. R. Theodoro, C. D. Machado Filho, M. F. Gama, J. P. Tardivo, F. M. Paschoal, and M. A. Pinhal, Clin. Exp. Dermatol. **37**(5), 527–533 (2012).
[44]K. Orth, G. Beck, F. Genze, and A. Ruck, J. Photochem. Photobiol., B **57**(2–3), 186–192 (2000).
[45]J. P. Tardivo, A. Del Giglio, C. S. de Oliveira, D. S. Gabrielli, H. C. Junqueira, D. B. Tada, D. Severino, R. de Fatima Turchiello, and M. S. Baptista, Photodiagn. Photodyn Ther. **2**(3), 175–191 (2005).
[46]A. Amirshaghaghi, L. Yan, J. Miller, Y. Daniel, J. M. Stein, T. M. Busch, Z. Cheng, and A. Tsourkas, Sci. Rep. **9**(1), 2613 (2019).
[47]D. Xu, A. Baidya, K. Deng, Y. S. Li, B. Wu, and H. B. Xu, Oncol. Rep. **45**(2), 547–556 (2021).
[48]P. Kumari, S. V. K. Rompicharla, H. Bhatt, B. Ghosh, and S. Biswas, Nanomedicine **14**(7), 819–834 (2019).
[49]B. Kramer and J. Bosman (2019). "Open access potential and uptake in the context of Plan S—A partial gap analysis," Zenodo, Dataset https://doi.org/10.5281/zenodo.10730837